医薬品 研究報告 調査報告書

識別番号・報告回数			報告日	第一報入手日	新医薬品等の区分	機構処理欄
				2006. 2. 21	該当なし	

一般的名称	新鮮凍結人血漿	研究報告の公表状況		公表国
販売名(企業名)	新鮮凍結血漿「日赤」(日本赤十字社)		Vabret A, Dina J, Gouarin S, Petitjean J, Corbet S, Freymuth F. Clin Infect Dis. 2006 Mar 1;42(5):634-9. Epub 2006 Jan 24.	フランス

研究報告の概要

○新規ヒトコロナウイルスHKU1の検出:6例の症例報告
背景:新規の第2群コロナウイルスであるヒトコロナウイルスHKU1(HCoV-HKU1)は、2005年に初めて香港の成人肺炎患者2名から同定された。著者らの知る限り、これまでにこの新規ウイルスの検出に関する報告はない。HCoV-HKU1の検出を可能にする分子学的方法、また6名の感染患者の臨床所見について報告する。
方法:2005年2月～3月に著者らの研究施設で135名の入院患者(5歳未満61.5%、20歳以上34.1%)から入手した141検体(135鼻腔検体及び6糞便検体)について、HCoV-HKU1スクリーニング検査を行った。
結果:HCoV-HKU1は、135鼻腔検体中6検体(4.4%)、6糞便検体中2検体(33.3%)で検出された。陽性となったのは、6名の患者(小児5名及び成人1名)由来の検体であった。6名の臨床所見は次の通りであった。3名は急性腸疾患のため脱水症状を起こして入院し、上気道炎も発症していた。1名は発熱、耳炎、熱けいれんを発症。1名は成長障害の調査のため検体を入手。1名はX連鎖無ガンマグロブリン血症及び白血球増加症の原因究明のため検体を入手した。
結論:HCoV-HKU1は、香港以外の一部地域において小児及び成人の呼吸器検体及び糞便検体から検出可能である。著者らの結果により、HCoV-HKU1は呼吸器及び腸疾患に関連する可能性があり、状態の不良な患者における持続性の無症候性感染との関連が考えられる。

報告企業の意見	今後の対応
新規ヒトコロナウイルスHKU1は呼吸器及び腸疾患に関連する可能性があり、状態の不良な患者における持続性の無症候性感染との関連が考えられるとの報告である。	今後も引き続き、新たなウイルス等による感染症の発生状況等に関する情報の収集に努める。

使用上の注意記載状況・その他参考事項等

新鮮凍結血漿「日赤」

血液を介するウイルス、細菌、原虫等の感染
vCJD等の伝播のリスク

(5)

MAJOR ARTICLE

Detection of the New Human Coronavirus HKU1: A Report of 6 Cases

Astrid Vabret,[1] Julia Dina,[1] Stéphanie Gouarin,[1] Joëlle Petitjean,[1] Sandrine Corbet,[1] and François Freymuth[1]

Laboratory of Virology, University Hospital of Caen, Caen, France

Background. Human coronavirus HKU1 (HCoV-HKU1), a new group 2 coronavirus, was first characterized in 2005 from 2 adults with pneumonia in Hong Kong, China. To the best of our knowledge, there is no other report to date about the detection of this new virus. We report a molecular method allowing for the detection of HCoV-HKU1 and also report the clinical presentation of 6 infected patients.

Methods. We screened 141 specimens (135 nasal samples and 6 stool samples) received in February and March 2005 in our laboratory and obtained from 135 hospitalized patients (61.5% of whom were <5 years old and 34.1% of whom were >20 years old) for HCoV-HKU1.

Results. HCoV-HKU1 was detected in 6 (4.4%) of the 135 nasal specimens and in 2 (33.3%) of the 6 stool samples; the positive samples were obtained from 6 patients (5 children and 1 adult). The clinical presentation of these 6 patients was as follows: 3 were admitted to the hospital for acute enteric disease resulting in severe dehydration associated with upper respiratory symptoms; 1 had fever, otitis, and febrile seizure; 1 had a sample obtained to investigate failure to thrive; and 1 had a sample obtained for exploration of X-linked agammaglobulinemia and hyperleucocytosis.

Conclusion. HCoV-HKU1 can be detected in respiratory and stool samples from children and adults in a part of the world other than Hong Kong. Our results suggest that HCoV-HKU1 could be associated with respiratory and enteric diseases, and its detection can be related to a persistent asymptomatic infection in patients with poor underlying conditions.

Coronaviruses (family *Coronaviridae*, order *Nidovirales*) are enveloped viruses with a linear, nonsegmented, positive-sense, single-stranded RNA genome and are divided into 3 distinct groups (group 1, group 2, and group 3). Five types of human coronaviruses (HCoV) have been described: HCoV-OC43 and HCoV-229E have been recognized since the mid-1960s and belong to group 1 and group 2. In 2003, the severe acute respiratory syndrome (SARS)–associated coronavirus (SARS-CoV) was identified, but it has not yet been assigned to one of the groups [1]. In 2004, another group 1 coronavirus, HCoV-NL63, was reported in The Netherlands [2, 3]. In January 2005, a new group 2 coronavirus, HCoV-HKU1, was found in 2 patients with pneumonia in Hong Kong. This new coronavirus was detected by RT-PCR of the *pol* gene of coronaviruses with use of conserved primers in the nasopharyngeal aspirates of patients. The complete genome was sequenced, and its general organization concurs with those of other coronaviruses. It contains the HE gene, which characterizes the group 2 coronaviruses, and has a very intriguing feature consisting of a variable number of tandem copies of a 30-bp repeat region that codes for a highly acidic domain (ATR) in ORF1a (nsp1 region). Despite the high number of cell cultures inoculated with respiratory samples, HCoV-HKU1 could not be recovered from cell culture [4]. No cytopathic effect was observed, and RT-PCR performed on the culture supernatant and cell lysates showed a lack of viral replication. Isolating HCoV on cell culture is very difficult. HCoV prototype strains 229E, OC43, and NL63 can replicate in MRC5 cells, HRT18 cells, and LLC-MK2 cells, respectively, but there are still few primary isolates. Woo et al. [4] reported that SARS-CoV can be recovered only from <20% of patients infected with SARS-CoV. There is no other report to date concerning the detection of HCoV-HKU1. In our laboratory, we conducted a preliminary study of 135 re-

Received 22 July 2005; accepted 4 October 2005; electronically published 24 January 2006.

Reprints or correspondence: Dr. Astrid Vabret, Laboratory of Virology, University Hospital of Caen, Ave. Georges Clemenceau, 14 033 Caen cedex, France (vabret-a@chu-caen.fr).

Clinical Infectious Diseases 2006; 42:634–9

1058-4838/2006/4205-0008$15.00

spiratory samples to know if this new coronavirus can be detected in a part of the world other than Hong Kong. The purpose of this article is to present the method used for the detection of HCoV-HKU1 and report the clinical presentation associated with this infection.

MATERIALS AND METHODS

We screened arbitrarily for HCoV-HKU1 135 HUH7 cell culture showing an extensive lysis at day 4 after onset of infection. HUH7 cells were inoculated with respiratory samples collected from 135 patients hospitalized in February and March 2005 at the University Hospital of Caen (Caen, France). The age distribution of the tested patients was as follows: 83 patients (61.5%) were <5 years of age, 6 patients (4.4%) were 6–20 years of age, and 46 patients (34.1%) were >21 years of age. The tested respiratory specimens were obtained from patients with respiratory symptoms and then were sent to the laboratory for viral diagnosis. The patients or, in the case of minors, the parents or legal guardians of the patients consented to having their samples tested for respiratory viruses, including coronaviruses. The samples were processed routinely for immunofluorescence direct antigen assay using monoclonal antibodies against influenza A and B viruses; respiratory syncytial virus; parainfluenzavirus types 1, 2, and 3; and adenovirus (Imagen). All samples had negative results. It is part of our strategy to inoculate samples with negative results onto a cell culture system (HUH7 cell line) [5]. In this protocol, HuH7 cells were grown in RPMI-1640 medium with glutamine with 5% fetal calf serum (Gibco; Invitrogen), penicillin (100 U/mL), and gentamycin (50 μg/mL), and were distributed in 48-well tissue culture microplates. When HUH7 cells were 80% confluent, the growth medium was discarded and each well was inoculated with 100 μL of the clinical samples. Microplates were centrifugated at 1500 rpm for 30 min at 30°C. Samples were then removed, and each well was filled with 1 mL of the same culture medium supplemented with 2% fetal calf serum (Gibco; Invitrogen). By day 4 after onset of infection, HuH7 cells were examined for cytopathic effect and the supernatant were used for amplification techniques. Cytopathic effect characteristics are as follows: small cells, no refringent, cells scattered on the culture, and a progressive lysis of the cell sheet. The RNA was extracted using the High pure RNA isolation kit (Roche) and tested with RT-PCR techniques previously described and used for the detection of rhinovirus, enterovirus, influenza virus C, HCoV-229E, HCoV-OC43, and HCoV-NL63 [6, 7]. A 1-step HCoV-HKU1 RT-PCR amplification of a 443-bp fragment was performed using the OneStep RT-PCR kit (Qiagen) and the following primers set defined in N gene from the GenBank sequence database (accession number AY597011): HKU1 sens (5′-ACCAATCTGAGCGAAATTACCAAAC-3′) and HKU1 antisense (5′-CGGAAACCTAGTAGGGATAGCTT-3′). The reaction was undertaken using OneStep RT-PCR kit (Qiagen, Courtaboeuf) according to the manufacturer's protocol. Each RT-PCR test was performed using the usual precautions to avoid contamination. No cross-reaction of this RT-PCR assay was observed with the other classical HCoV. The assay was performed without a positive control. RT-PCR products were processed on an agarose gel stained with ethidium bromide and visualized under UV light. The positive results were confirmed by sequencing from the amplified product and by RT-PCR performed directly with use of the respiratory specimens. For 2 patients with results positive for detection of HCoV-HKU1 in respiratory specimens, stool samples obtained at the same time were available and have been tested. Two other RT-PCR assays were performed using the specimen that was positive for HCoV-HKU1 detection, one of which involved amplification of a 713-bp fragment with S1 gene–specific primers HKU1-S1 sens (5′-ACCACAGTTCCTCGCATAAGT-3′) and HKU1-S1 antisense (5′-AGATATTGGCGTTTAGAC-3′), the other amplifying a variable size fragment with primers defining on both sides of the highly acidic domain in ORF1a (ATR-HKU1 sens: 5′-AATGGCCTCTCGTATGTAT-3′; ATR-HKU1 antisense: 5′-TTACAAGTAACACAGAACGCA-3′). The RT-PCR products were sequenced, and the obtained nucleotide sequences of the partial S1 gene were compared with the prototype strain sequences available in GenBank. The alignments were prepared using Clustal X, version 1.83. A phylogenetic tree was constructed by the neighbor-joining method, and bootstrap values were determined by 1000 replicates. We used HCoV-OC43 as an outgroup. The medical records were examined retrospectively for the 6 patients with test results positive for HCoV-HKU1.

RESULTS

Among the 135 cell cultures tested with RT-PCR, the positive samples consisted of 10 coronaviruses (6 positive for HCoV-HKU1, 2 positive for HCoV-NL63, and 2 positive for HCoV-OC43), 23 rhinoviruses, 1 enterovirus, and 1 influenza virus C. There were 2 codetections, one of which consisted of HCoV-HKU1 and influenza virus C, and the other of which consisted of rhinovirus and HCoV-OC43. To eliminate cell culture contamination, the N gene HCoV-HKU1 RT-PCR was performed directly on the respiratory specimens obtained from the 6 patients. All of these specimens, as well as the stool samples available for 2 of these patients, were found to have positive results. The 443-bp amplicon resulting from the amplification of the partial N gene was sequenced for 6 of the 8 specimens with positive results (GenBank accession numbers DQ131635–DQ131641) (figure 1). Our isolates shared 98%–100% nucleotide identity with the same region of the HCoV-HKU1 reference strain. We then sequenced the 713-bp amplicon corresponding to partial spike gene of 4 positive specimens.

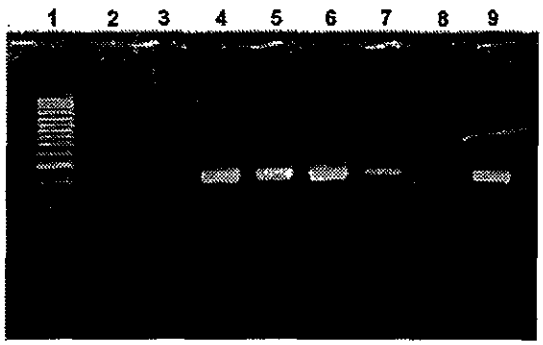

Figure 1. Ethidium bromide stain of 2% agarose gel showing RT-PCR products (443 bp) of partial coronavirus N gene with human coronavirus HKU1–specific primers. *Lane 1,* size marker (100 bp); *lanes 2, 4–7,* and *9,* positive respiratory samples; *lanes 3* and *8,* negative control RT-PCR mix.

Genetic sequences from other positive specimens could not be obtained, because the primers used for the amplification of the partial spike gene did not amplify a PCR product of sufficient quantity to allow for reliable genetic sequencing analysis. The phylogenetic analysis of 603-bp of these sequences (GenBank accession numbers DQ131642–DQ131645) shows that our isolates form a group containing sequences with different markers and that there is no cross-contamination between the different isolates. Three of these isolates clustered with the prototype strain described in Hong Kong. One isolate (DQ131645) had characteristics of an outlier (figure 2). To determine if our isolates contained a variable number of tandem copies of 30-bp repeat region—the significant feature of HCoV-HKU1—we sequenced amplicon resulting from a RT-PCR of the region of ORF1a. To confirm the number of ATRs, this test was conducted several times for 2 isolates. The results show that there were 7 and 8 ATRs in the 2 isolates tested, compared with 11 and 14 ATRs recorded in the 2 Hong Kong isolates [4].

HCoV-HKU1 was detected in nasal and stool samples obtained from 6 patients, 4 of whom were male, and 2 of whom were female (table 1). The age of the infected patients ranged from 8 months to 5 years, with the exception of one 19-year-old man (patient 5). The age distribution of the patients infected with HCoV-HKU1 and the age distribution of tested patients were closed. The medical records of all 6 patients were examined. Three of them (patients 1, 2, and 6) were admitted to the hospital for severe dehydration due to fever, vomiting, and diarrhea. Upper respiratory symptoms (rhinitis, pharyngitis, or otitis) were also reported. Unfortunately, no stool samples for these patients were available in the hospital. Patient 4 had a febrile seizure and otitis. Both respiratory and stool samples tested positive for HCoV-HKU1. Patients 3 and 5 were admitted to the hospital for a complete investigation and did not suffer from acute symptoms; patient 3 was an 8-month-old girl with failure to thrive, and patient 5 was a 19-year-old man with Bruton agammaglobulinemia and hyperleucocytosis with a final diagnosis of chronic myeloid leukaemia. A stool sample obtained from patient 3 was available and tested positive for HCoV-HKU1.

DISCUSSION

HCoV-HKU1 was first characterized in Hong Kong in January 2005 in the respiratory specimens of 2 adults with pneumonia. HCoV-HKU1 is a previously unrecognized group 2 coronavirus. The clinical significance of this viral infection was made evident in the index patient by the combined evolution of clinical symptoms, viral loads in the respiratory samples, and development of a specific antibody response. This index patient was a 71-year-old Chinese man with poor underlying conditions (pulmonary tuberculosis complicated by bronchiectasis, a history of being a chronic smoker, and obstructive airway disease). He was admitted to the hospital for pneumonia and was discharged after 5 days of hospitalization. However, respiratory, stool, and urine samples were collected from him weekly for a 5-week period. The viral load in respiratory specimens decreased during the second week of the illness and was undetectable in the third week. The decrease in viral load was accompanied by recovery from the illness and development of a specific antibody response. HCoV-HKU1 was detected only in respiratory specimens, not in stool and urine samples [4]. There is no other report to date about the geographic and temporal distribution and the clinical symptoms associated with this virus.

In our study, the arbitrary decision was made to screen 135 HUH7 cell cultures showing a cytopathic effect at day 4 after onset of infection and inoculated by nasal specimens collected during 2 winter months, February and March 2005. The choice of HUH7 cells was made because some studies showed that these cells appear to have a broad spectrum, allowing for the detection of a wide range of viruses, including coronaviruses 229E, OC43, and MHV [8–10]. Unfortunately, we failed to amplify HCoV-HKU1 on HUH7 cells by serial passage. At first passage, we could see a cytopathic effect on day 4. However, because of the lack of specific antibodies against HCoV-HKU1, we could not test HUH7 cells to know whether there were infected cells showing viral replication. So, the HCoV-HKU1 RNA detected by RT-PCR may be a residual virus from a clinical sample or a virus amplified in cell culture in the first passage on HUH7 cells. The duration of incubation is limited to 4 days, which may be insufficient for the growth of coronaviruses. More experiments are being conducted to adapt HKU1 strains to cell line. Six patients were infected with HCoV-HKU1, including 5 children and 1 adult. Because samples were obtained mainly from pediatric departments, 61.5% of the tested patients were children. So, the high frequency with which HCoV-HKU1

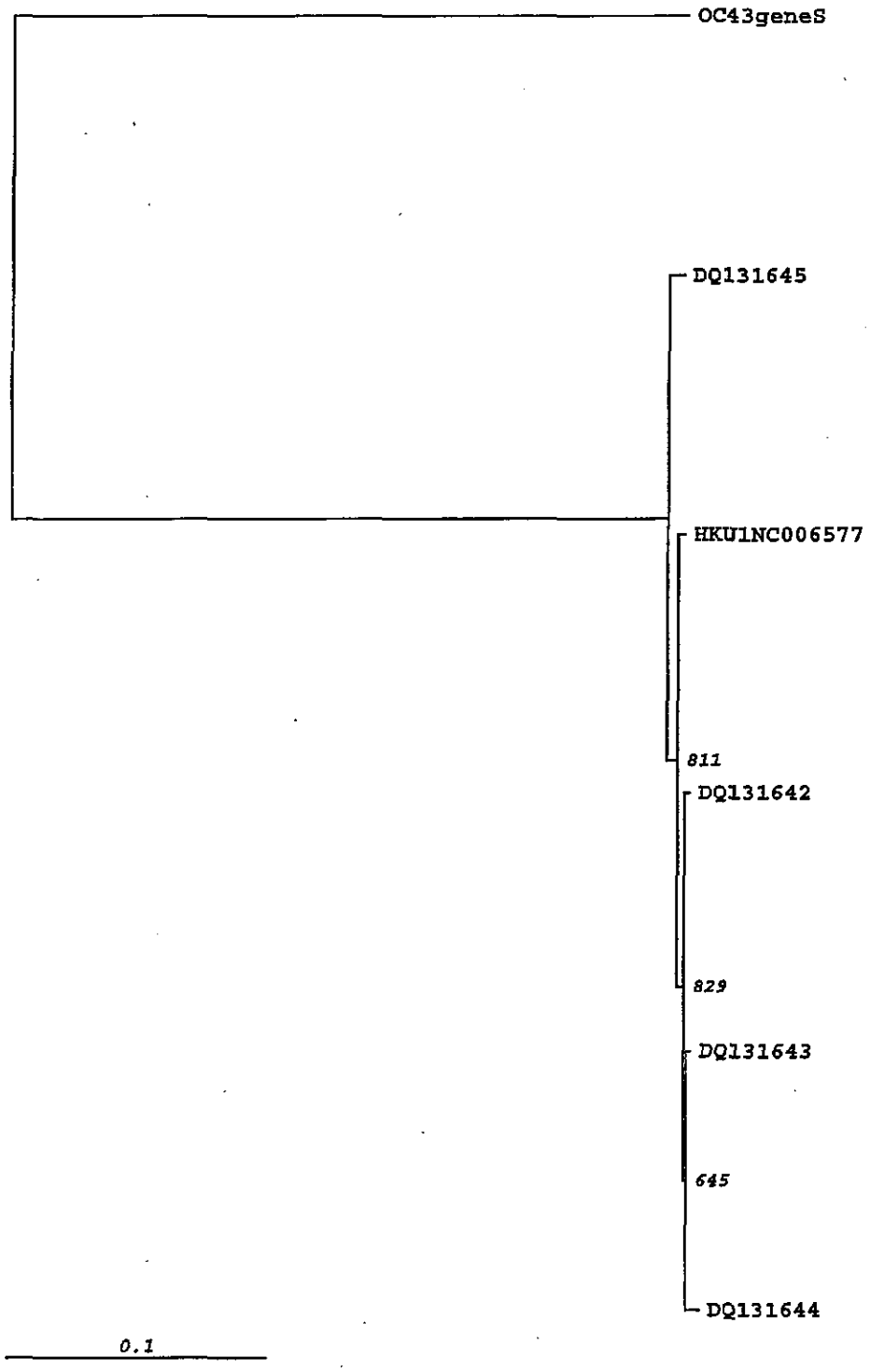

Figure 2. Phylogenetic analysis of a 603-bp region of partial spike gene of 4 human coronavirus (HCoV)–HKU1 isolates from France. The phylogenetic tree was constructed by the neighbor-joining method, and bootstrap values were determined by 1000 replicates in Clustal X, version 1.83. To construct the tree, the reference strain HCoV-HKU1 (NC006577) was included. HCoV-OC43 is used as the outgroup.

Table 1. Clinical presentation of patients infected with human coronavirus HKU1.

Patient	Sample date	Age/sex	Medical history	Symptom(s)	Diagnosis	Stool sample
1	14 February 2005	3 years/F	None	Fever (temperature, 38°3), vomiting, diarrhea, rhinitis, otitis	Gastroenteritis, dehydration	Not tested
2	5 February 2005	5 years/M	None	Fever (temperature, 39°3), vomiting, diarrhea, weight loss	Gastroenteritis, dehydration	Not tested
3	4 March 2005	8 months/F	In uterine growth retardation	Failure to thrive	Full investigation	Positive for HKU1
4	7 March 2005	18 months/M	Atopic dermatitis and bronchiolitis	Fever, otitis, convulsions	Febrile seizure	Positive for HKU1
5	11 March 2005	19 years/M	Bruton disease and bronchiectasis	Hyperleucocytosis (WBC count, 54,000 cells/mm^3)	Chronic myeloid leukemia	Not tested
6[a]	29 March 2005	9 months/M	None	Fever (temperature, 39°C), vomiting, diarrhea, rhinitis, pharyngitis	Severe dehydration	Not tested

[a] Patient was coinfected with human coronavirus HKU1 and influenza C virus.

was detected in children was biased because of the recruitment of the samples. There is no evidence that children are more commonly infected by HCoV-HKU1 than other individuals. Positive specimens were collected throughout the study period, from 14 February to 24 March 2005. This distribution did not indicate an outbreak. HCoV strains OC43, 229E, and NL63 are reported to have a winter seasonality in temperate regions [2, 8, 9, 10]. Our study only suggests that HCoV-HKU1 could also have a winter seasonality in these regions. A better understanding of the epidemiology of different HCoV in different parts of the world could contribute to better management of the molecular and serological diagnosis of future emerging or reemerging viruses, such as SARS-CoV. Because of the lack of a systematized selection of the tested samples, the patients with positive results are presented as case reports.

It should be noted that one-half of the patients were admitted to the hospital not for respiratory illnesses, but for gastroenteritis resulting in severe dehydration associated with upper respiratory symptoms. In effect, previous studies have suggested that coronaviruses other than SARS-CoV may be involved in enteric diseases, despite the fact that there is no clear evidence that they cause enteric illness [9, 11–13]. This would not be surprising in view of the clear involvement of SARS-CoV and some animal coronavirus strains in severe diarrheal diseases. We have shown that HCoV-HKU1 can be detected in stool samples. Nevertheless, further studies must be conducted to confirm the potential dual tropism (respiratory and enteric) of this group 2 coronavirus.

HCoV-HKU1 was also detected in 2 patients without acute symptoms and with poor underlying conditions (patients 3 and 5). Although HCoV (except SARS-CoV) were generally associated with acute and self-limiting respiratory infections, this detection of viral RNA can be related to a persistent or asymptomatic chronic infection. Chiu et al. [14] reported a repeated detection of HCoV-229E in an immunocompromised child >3 months old. The genetic analysis of a 305-bp region of the spike protein region of 229E revealed that these 3 specimens had identical genetic sequences, providing evidence of virus persistence rather than reinfection. Patient 6, who tested positive for HCoV-HKU1, had an influenza C virus detected in the same clinical specimen. It is not possible to determine whether this is true coinfection or whether 1 of the viruses represents continued shedding from a previous infection. It is interesting to note that the genome of group 2 coronaviruses and influenza C virus both contain the HE gene. Phylogenetic analysis suggested that the HE genes of coronaviruses and influenza C have a common ancestral origin. Because HCoV and influenza C virus infect similar tissues, the significant sequence homology between the HE genes of the 2 viruses suggests that coinfection followed by recombination could have occurred in the past [4, 15]. The expression of the HE gene has been shown to be heterogeneous in different species of group 2 coronaviruses. The biological significance of HE protein is not well understood. Further experiments have to be performed to determine the essentiality and function of HE in HCoV-HKU1, especially in cell tropism.

In conclusion, we report a molecular method allowing for the detection of the new coronavirus HKU1. We are able to detect HKU1 in respiratory samples and stool specimens, indicating that this virus can be excreted in this way. Our results indicate that HCoV-HKU1 is present in hospitalized patients with mild respiratory and enteric tract illness. Determining whether or not HCoV-HKU1 can cause enteric diseases will require further investigations. Phylogenetic analysis of our isolates suggest that both variants of HCoV-HKU1 may cocirculate. Ours is the first observation and report of HCoV-HKU1 infection in France. Future studies will yield more-accurate data about the circulation of this virus.

Acknowledgments

Potential conflicts of interest. All authors: no conflicts.

Financial support. The European Commission EPISARS contract (SP22-CT-2004-511063) and the Programme de Recherche en Réseaux Franco-Chinois (épidémie du SRAS : de l'émergence au contrôle).

References

1. Gorbalenya AE, Snijder EJ, Spaan WJ. Severe acute respiratory syndrome coronavirus phylogeny: toward consensus. J Virol 2004; 78: 7863–6.
2. Van der Hoek L, Pyrc K, Jebbink MF, et al. Identification of a new human coronavirus. Nat Med 2004; 10:368–73.
3. Fouchier RA, Hartwig NG, Bestebroer TM, et al. A previously undescribed coronavirus associated with respiratory disease in humans. Proc Natl Acad Sci USA 2004; 101:6212–6.
4. Woo PC, Lau SK, Chu CM, et al. Characterization and complete genome complete sequence of a novel coronavirus, coronavirus HKU1, from patients with pneumonia. J Virol 2005; 79:884–95.
5. Freymuth F, Vabret A, Rozenberg F, et al. Replication of respiratory viruses, particularly influenza virus, rhinovirus, and coronavirus in HUH7 hepatocarcinoma cell line. J Med Virol 2005; 77:295–301.
6. Bellau-Pujol S, Vabret A, Legrand L, et al. Development of three multiplex RT-PCR assays for the detection of 12 respiratory RNA viruses. J Virol Methods 2005; 126:53–63.
7. Vabret A Mourez T, Dina J, et al. Human coronavirus NL63, France. Emerg Infect Dis 2005; 11:1225–9.
8. Koetters PJ, Hassanieh L, Stohlman SA, Gallagher T, Lai MMC. Mouse hepatitis virus strain JHM infects a human hepatocellular carcinoma cell line. Virology 1999; 264:398–409.
9. Pene F, Merlat A, Vabret A, et al. Coronavirus 229E-related pneumonia in immunocompromised patients. Clin Infect Dis 2003; 37:929–32.
10. Vabret A, Mourez T, Gouarin S, Petitjean J, Freymuth F. An outbreak of coronavirus OC43 respiratory infection in Normandy, France. Clin Infect Dis 2003; 36:985–9.
11. Bastien N, Robinson JL, Tse A, Lee BE, Hart L, Li Y. Human coronavirus NL-63 infections in children: a 1-year study. J Clin Microbiol 2005; 43:4567–73.
12. Zhang XM, Herbst W, Kousoulas KG, Storz J. Biological and genetic characterization of a hemagglutinating coronavirus isolated from a diarrhoeic child. J Med Virol 1994; 44:152–61.
13. Chany C, Moscovici O, Lebon P, Rousset S. Association of coronavirus infection with neonatal necrotizing enterocolitis. Pediatrics 1982; 69: 209–14.
14. Chiu SS, Chan KH, Chu KW, et al. Human coronavirus NL63 infection and other coronavirus infections in children hospitalized with acute respiratory disease in Hong Kong, China. Clin Infect Dis 2005; 40: 1721–9.
15. Zhang XM, Kousoulas KG, Storz J. The hemagglutinin/esterase gene of human coronavirus strain OC43: phylogenetic relationships to bovine and murine coronaviruses and influenza C virus. Virology 1992; 186:318–23.

別紙様式第2-1

No. 17

医薬品 研究報告 調査報告書

識別番号・報告回数			報告日	第一報入手日	新医薬品等の区分	機構処理欄
				2005. 11. 24	該当なし	

一般的名称	人血清アルブミン	研究報告の公表状況	Li W, Shi Z, Yu M, Ren W, Smith C, Epstein JH, Wang H, Crameri G, Hu Z, Zhang H, Zhang J, McEachern J, Field H, Daszak P, Eaton BT, Zhang S, Wang LF. Science. 2005 Oct 28;310(5748):676-9. Epub 2005 Sep 29.	公表国
販売名(企業名)	赤十字アルブミン20(日本赤十字社) 赤十字アルブミン25(日本赤十字社)			中国

研究報告の概要

○コウモリはSARS様コロナウイルスの自然宿主である
2002年から2003年にかけて、中国南部で重症急性呼吸器症候群(SARS)が出現した。その病原体であるSARSコロナウイルス(SARS-CoV)の起源は依然として理解されていない。本稿では、ある種のコウモリがSARS発生の原因であるコロナウイルスに密接に関連するコロナウイルスの自然宿主であることを報告する。SARS様コロナウイルス(SL-CoV)と呼ばれるこれらのウイルスは、ヒトやジャコウネコから分離されたSARS-CoVより遺伝的多様性が高い。ヒト及びジャコウネコからのSARS-CoV分離株は系統発生学的にSL-CoVの範疇に入り、SARS発生の原因ウイルスがこのコロナウイルス群の一員であったことが示される。

報告企業の意見	今後の対応
コウモリがSARS様コロナウイルスの自然宿主であることが判明したとの報告である。	コロナウイルスは脂質膜を持つRNAウイルスである。これまで、本製剤によるコロナウイルス感染の報告はない。本製剤の製造工程には、平成11年8月30日付医薬発第1047号に沿ったウイルス・プロセスバリデーションによって検証された2つの異なるウイルス除去・不活化工程が含まれていることから、本製剤の安全性は確保されていると考えるが、念のため今後も情報収集に努める。

使用上の注意記載状況・その他参考事項等

赤十字アルブミン20
赤十字アルブミン25

血液を原料とすることに由来する感染症伝播等

(ほ)

8. W. D. Lawton, M. J. Surgalla, *J. Infect. Dis.* 113, 39 (1963).
9. A. V. Philipovskiy *et al.*, *Infect. Immun.* 73, 1532 (2005).
10. T. Kubori *et al.*, *Science* 280, 602 (1998).
11. F. S. Cordes *et al.*, *J. Biol. Chem.* 278, 17103 (2003).
12. E. Hoiczyk, G. Blobel, *Proc. Natl. Acad. Sci. U.S.A.* 98, 4669 (2001).
13. L. Journet, C. Agrain, P. Broz, G. R. Cornelis, *Science* 302, 1757 (2003).
14. *Yersinia* builds injectisomes when the temperature reaches 37°C, the host's body temperature. Yop secretion is triggered by contact with a target cell or artificially by chelation of Ca^{2+} ions (15).
15. Materials and methods are available as supporting material on *Science* Online.
16. Removal of *lcrV* leads to reduced synthesis of YopB and YopD because of a regulatory effect of LcrV on their expression. This undesired effect can be compensated by deleting *yopQ* (5).
17. C. A. Mueller *et al.*, unpublished data.
18. W. L. Picking *et al.*, *Infect. Immun.* 73, 1432 (2005).
19. S. J. Daniell *et al.*, *Cell. Microbiol.* 3, 865 (2001).
20. D. Chakravortty, M. Rohde, L. Jager, J. Deiwick, M. Hensel, *EMBO J.* 24, 2043 (2005).
21. We thank P. Jenő for mass spectrometry analyses, M. Duerrenberger for use of the TEM facility, and J. M. Meyer and J. Frey for supplying *P. aeruginosa* PAO1 and *A. salmonicida* JF2267. Supported by the Swiss National Science Foundation (grant nos. 32-65393.01 to G.C. and 3100-059415 to A.E.) and by the Maurice E. Müller Foundation of Switzerland.

Supporting Online Material
www.sciencemag.org/cgi/content/full/310/5748/674/DC1
Materials and Methods
Figs. S1 to S8
Tables S1 and S2
References and Notes

5 August 2005; accepted 4 October 2005
10.1126/science.1118476

Bats Are Natural Reservoirs of SARS-Like Coronaviruses

Wendong Li,[1,2] Zhengli Shi,[2]* Meng Yu,[3] Wuze Ren,[2] Craig Smith,[4] Jonathan H. Epstein,[5] Hanzhong Wang,[2] Gary Crameri,[3] Zhihong Hu,[2] Huajun Zhang,[2] Jianhong Zhang,[2] Jennifer McEachern,[3] Hume Field,[4] Peter Daszak,[5] Bryan T. Eaton,[3] Shuyi Zhang,[1,6]* Lin-Fa Wang[3]*

Severe acute respiratory syndrome (SARS) emerged in 2002 to 2003 in southern China. The origin of its etiological agent, the SARS coronavirus (SARS-CoV), remains elusive. Here we report that species of bats are a natural host of coronaviruses closely related to those responsible for the SARS outbreak. These viruses, termed SARS-like coronaviruses (SL-CoVs), display greater genetic variation than SARS-CoV isolated from humans or from civets. The human and civet isolates of SARS-CoV nestle phylogenetically within the spectrum of SL-CoVs, indicating that the virus responsible for the SARS outbreak was a member of this coronavirus group.

Severe acute respiratory syndrome (SARS) was caused by a newly emerged coronavirus, now known as SARS coronavirus (SARS-CoV) (*1*, *2*). In spite of the early success of etiological studies and molecular characterization of this virus (*3*, *4*), efforts to identify the origin of SARS-CoV have been less successful. Without knowledge of the reservoir host distribution and transmission routes of SARS-CoV, it will be difficult to prevent and control future outbreaks of SARS.

Studies conducted previously on animals sampled from live animal markets in Guangdong, China, indicated that masked palm civets (*Paguma larvata*) and two other species had been infected by SARS-CoV (*5*). This led to a large-scale culling of civets to prevent further SARS outbreaks. However, subsequent studies have revealed no widespread infection in wild or farmed civets (*6*, *7*). Experimental infection of civets with two different human isolates of SARS-CoV resulted in overt clinical symptoms, rendering them unlikely to be the natural reservoir hosts (*8*). These data suggest that although *P. larvata* may have been the source of the human infection that precipitated the SARS outbreak, infection in this and other common species in animal markets was more likely a reflection of an "artificial" market cycle in naïve species than an indication of the natural reservoir of the virus.

Bats are reservoir hosts of several zoonotic viruses, including the Hendra and Nipah viruses, which have recently emerged in Australia and East Asia, respectively (*9*–*11*). Bats may be persistently infected with many viruses but rarely display clinical symptoms (*12*). These characteristics and the increasing presence of bats and bat products in food and traditional medicine markets in southern China and elsewhere in Asia (*13*) led us to survey bats in the search for the natural reservoir of SARS-CoV.

In this study, conducted from March to December of 2004, we sampled 408 bats representing nine species, six genera, and three families from four locations in China (Guangdong, Guangxi, Hubei, and Tianjin) after trapping them in their native habitat (Table 1). Blood, fecal, and throat swabs were collected; serum samples and cDNA from fecal or throat samples were independently analyzed, double-blind, with different methods in our laboratories in Wuhan and Geelong (*14*).

Among six genera of bat species surveyed (*Rousettus*, *Cynopterus*, *Myotis*, *Rhinolophus*, *Nyctalus*, and *Miniopterus*), three communal, cave-dwelling species from the genus *Rhinolophus* (horseshoe bats) in the family *Rhinolophidae* demonstrated a high SARS-CoV antibody prevalence: 13 out of 46 bats (28%) in *R. pearsoni* from Guangxi, 2 out of 6 bats (33%) in *R. pussilus* from Guangxi, and 5 out of 7 bats (71%) in *R. macrotis* from Hubei. The high seroprevalence and wide distribution of seropositive bats is expected for a wildlife reservoir host for a pathogen (*15*).

The serological findings were corroborated by polymerase chain reaction (PCR) analyses with primer pairs derived from the nucleocapsid (N) and polymerase (P) genes (table S1). Five fecal samples tested positive, all of them from the genus *Rhinolophus*: three in *R. pearsoni* from Guangxi and one each in *R. macrotis* and *R. ferrumequinum*, respectively, from Hubei. No virus was isolated from an inoculation of Vero E6 cells with fecal swabs of PCR-positive samples.

A complete genome sequence was determined directly from PCR products from one of the fecal samples (sample Rp3) that contained relatively high levels of genetic material. The genome organization of this virus (Fig. 1), tentatively named SARS-like coronavirus isolate Rp3 (SL-CoV Rp3), was essentially identical to that of SARS-CoV, with the exception of three regions (Fig. 1, shaded boxes). The overall nucleotide sequence identity between SL-CoV Rp3 and SARS-CoV Tor2 was 92% and increased to ~94% when the three variable regions were excluded. The variable regions are located at the 5′ end of the S gene (equivalent to the S1 coding region of coronavirus S protein) and the region immediately upstream of the N gene. These regions have been identified as "high mutation" regions among different SARS-CoVs (*5*, *16*, *17*). The region upstream of the N gene is known to be prone to deletions of various sizes (*5*, *16*, *18*).

Predicted protein products from each gene or putative open reading frame (ORF) of SL-CoV Rp3 and SARS-CoV Tor2 were com-

[1]Institute of Zoology, Chinese Academy of Sciences (CAS), Beijing, China. [2]State Key Laboratory of Virology, Wuhan Institute of Virology, CAS, Wuhan, China. [3]Commonwealth Scientific and Industrial Research Organization (CSIRO) Livestock Industries, Australian Animal Health Laboratory, Geelong, Australia. [4]Department of Primary Industries and Fisheries, Queensland, Australia. [5]The Consortium for Conservation Medicine, New York, USA. [6]Guangzhou Institute of Biomedicine and Health, Guangzhou, China.

*To whom correspondence should be addressed. E-mail: zlshi@wh.iov.cn (Z.S.); zhangsy@ioz.ac.cn (S.Z.); linfa.wang@csiro.au (L.-F.W.)

Table 1. Detection of antibodies to SARS-CoV and PCR amplification of N and P gene fragments with SARS-CoV–specific primers. ND, not determined because of poor sample quality or unavailability of specimens from individual animals.

Sampling		Bat species	Antibody test: positive/total (%)	PCR analysis: positive/total (%)	
Time	Location			Fecal swabs	Respiratory swabs
Mar 04	Nanning, Guangxi	*Rousettus leschenaulti*	1/84 (1.2%)	0/110	ND
	Maoming, Guangdong	*Rousettus leschenaulti*	0/42	0/45	ND
		Cynopterus sphinx	0/17	0/27	ND
July 04	Nanning, Guangxi	*Rousettus leschenaulti*	ND	0/55	0/55
	Tianjin	*Myotis ricketti*	ND	0/21	0/21
Nov 04	Yichang, Hubei	*Rhinolophus pusillus*	ND	0/15	ND
		Rhinolophus ferrumequinum	0/4	1/8 (12.5%)*	ND
		Rhinolophus macrotis	5/7 (71%)	1/8 (12.5%)†	0/3
		Nyctalus plancyi	0/1	0/1	ND
		Miniopterus schreibersi	0/1	0/1	ND
		Myotis altarium	0/1	0/1	ND
Dec 04	Nanning, Guangxi	*Rousettus leschenaulti*	1/58 (1.8)	ND	ND
		Rhinolophus pearsoni	13/46 (28.3%)	3/30 (10%)‡	0/11
		Rhinolophus pussilus	2/6 (33.3%)	0/6	0/2

*Positive fecal sample designated Rf1 †Positive fecal sample designated Rm1 ‡Positive fecal samples designated Rp1, Rp2, and Rp3, respectively.

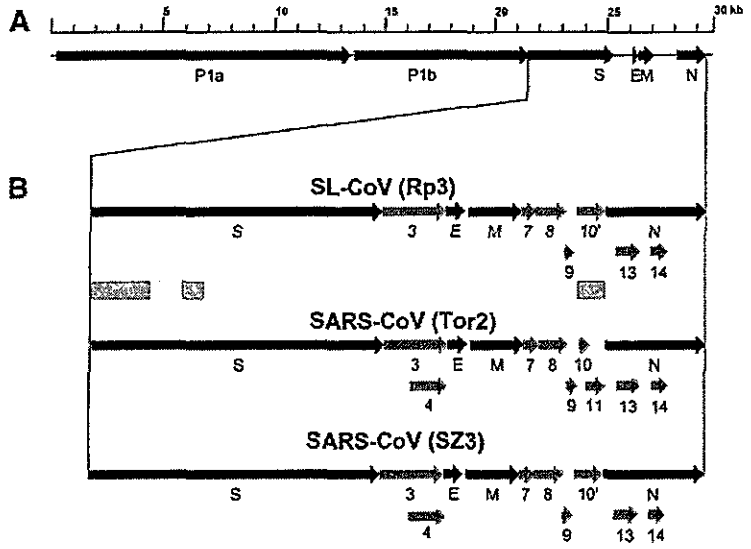

Fig. 1. Genome organization of, and comparison between, SL-CoV and SARS-CoV. (A) Overall genome organization of SL-CoV Rp3. (B) Expanded diagram of the 3′ region of the genome in comparison with SARS-CoV strains Tor2 and SZ3, following the same nomenclature used by Marra *et al.* (*4*). The genes (named by letters P, S, E, M, and N) present in all coronaviruses are shown in dark-colored arrows, whereas the SARS-CoV–specific ORFs are numbered and illustrated in light-colored arrows. ORF10′ follows the nomenclature by Guan *et al.* (*5*) to indicate that the single ORF present between ORF9 and N in SL-CoV is equivalent to the fusion of ORF10 and ORF11 in the same region in SARS-CoV Tor2. The shaded boxes mark the only three regions displaying significant sequence difference between the two viruses (table S2).

pared (table S2). The P, S, E, M, and N proteins, which are present in all coronaviruses, were similarly sized in the two viruses, with sequence identities ranging from 96% to 100%. The only exception was the S1 domain of the S protein, where sequence identity fell to 64%. The S1 domain is involved in receptor binding, whereas the S2 domain is responsible for the fusion of virus and host cell membranes (*19*). The sequence divergence in the S1 domain corroborated our serum neutralization studies, which indicated that although bat sera have a high level of cross-reactive antibodies (with enzyme-linked immunosorbent assay titers ranging from 1:100 to 1:6400), they failed to neutralize SARS-CoV when tested on Vero E6 cells. This finding suggests that S1 is the main target for antibody-mediated neutralization of this group of viruses, which is consistent with previous reports indicating that major SARS-CoV neutralization epitopes are located in the S1 region (*20, 21*).

In addition to the five genes present in all coronavirus genomes, coronaviruses also have several ORFs between the P gene and the 3′ end of the genome that code for nonstructural proteins. The function of these nonstructural proteins is largely unknown. The location and sequence of ORFs are group- or virus-specific and hence can serve as important molecular markers for studying virus evolution and classification (*19, 22*). SARS-CoV has a unique set of ORFs not shared by any of the known coronaviruses (*3, 4*). Most of these ORFs were also present in SL-CoV, confirming the extremely close genetic relationship between SARS-CoV and SL-CoV (Fig. 1 and table S2).

Coronaviruses produce subgenomic mRNAs through a discontinuous transcription process not fully characterized (*19*). Conserved nucleotide sequences functioning as transcription regulatory sequences (TRSs) are required for the production of the subgenomic mRNAs. In SARS-CoV, such TRSs were identified at each of the predicted gene start sites (*3, 4*). All of these TRSs were absolutely conserved between SARS-CoV Tor2 and SL-CoV Rp3 (table S3), further demonstrating that these two viruses are very closely related.

SL-CoV is completely different from a bat coronavirus (bat-CoV) recently identified by Poon *et al.* (*7*) from species of bats in the genus *Miniopterus* during a wildlife surveillance study in Hong Kong (Fig. 2). Because the complete genome sequence was not available for bat-CoV, only the trees covering the common sequences (i.e., parts of the P1b and S2 proteins) are shown. The phylogenetic analysis demonstrated that SL-CoV Rp3 and SARS-CoVs are clustered together but that bat-CoV is placed among the relatively distant group 1 viruses. Hereafter, SARS-CoVs and SL-CoVs will be collectively called the SARS cluster of coronaviruses.

In addition to the complete genome sequence of SL-CoV Rp3, partial genome sequences for the other four PCR-positive bat samples were also determined. Phylogenetic analysis based on the N protein sequences (Fig. 3A) revealed that the genetic variation among the SL-CoV sequences was much greater than that exhibited by SARS-CoVs (for simplicity, only three human and civet SARS-CoV isolates were used; the remainder are almost identical to those shown). This was especially obvious when SL-CoVs isolated from different bat species were compared. Moreover, the results suggested that SARS-CoVs nestle phylogenetically within the spectrum of SL-CoVs.

We also compared the "high mutation" regions in samples Rf1, Rm1, and Rp3. For the region upstream of the N gene, SL-CoVs from all three bat species contained a single ORF (ORF10′), similar to that found in SARS-CoV isolates from civets (*5*) and patients in the early phase of the outbreaks (*16, 18*) but different from that in most human isolates, which

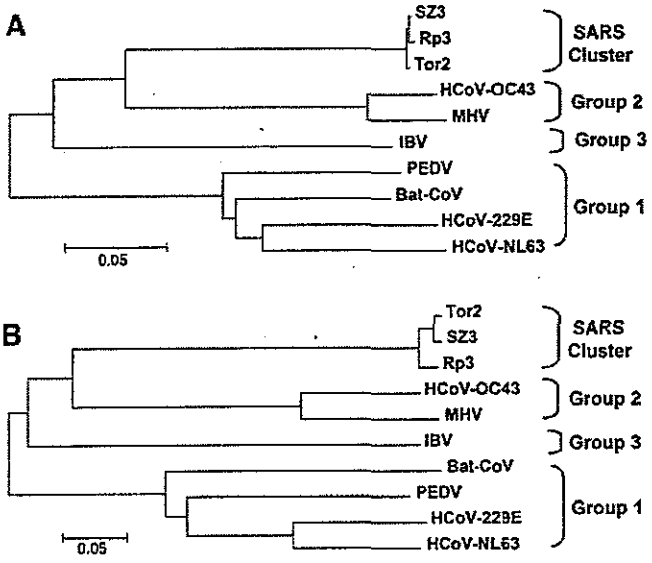

Fig. 2. Phylogenetic trees. (A) and (B) are trees based on deduced amino acid sequences of the same regions in P1b and S, respectively, as used by Poon *et al.* (*7*) for bat-CoV. Tor2 and SZ3, SARS-CoV strains Tor2 and SZ3; Rp3, SL-CoV Rp3; HCoV, human coronavirus; MHV, mouse hepatitis virus; PEDV, porcine epidemic diarrhea virus; IBV, avian infectious bronchitis virus.

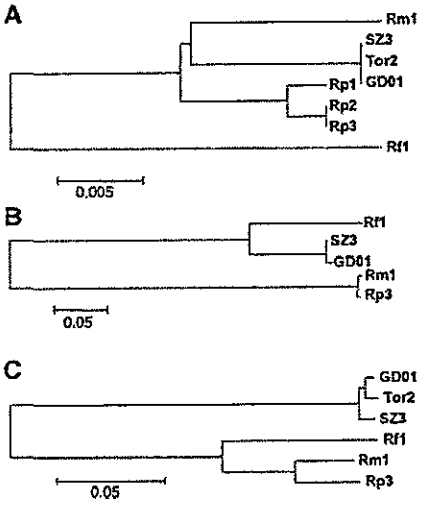

Fig. 3. Phylogenetic trees based on deduced amino acid sequences of (A) N, (B) ORF10′, and (C) S1 proteins. Tor2, SZ3, and GD01, different SARS-CoV strains; Rf1, Rm1, and Rp1-3, different SL-CoV sequences. The genetic distance scale shown for (A) is different from those for (B) and (C).

have a 29-nucleotide deletion in this region (*3*, *4*, *16*). ORF10′ in Rf1 codes for a protein having the same size (122 amino acids) as and more than 80% sequence identity to ORF10′ proteins of SARS-CoVs, but those in Rm1 and Rp3 code for a 121–amino acid protein with only 35% sequence identity (Fig. 3B and fig. S2). By contrast, analysis of the S1 protein regions (Fig. 3C and fig. S3) indicated that Rf1 was more closely related to SL-CoVs from two other bat species than to SARS-CoVs, suggesting that the SARS cluster of coronaviruses could recombine to increase genetic diversity and fitness, as is well documented for other coronaviruses (*19*). We were unable to sequence these regions for Rp1 or Rp2, owing to the poor quality of the fecal materials from these two animals. The limited amount of cDNA available was used up for N gene analysis and in initial sequencing trials with SARS-CoV–derived primers, which were largely unsuccessful. Judging from the close relationship of the N genes between Rp1, Rp2, and Rp3 (fig. S1), it is unlikely that Rp1 or Rp2 will have major sequence differences from Rp3 in the S1 or ORF10′ regions. This is not unexpected, considering that these three positive samples were obtained from the same bat species in the same location.

The genetic diversity of bat-derived sequences supports the notion that bats are a natural reservoir host of the SARS cluster of coronaviruses. A similar observation has been made for henipaviruses, another important group of emerging zoonotic viruses of bat origin, which show greater genetic diversity in bats than was observed among viruses isolated during the initial Nipah outbreaks in Malaysia (*23*–*26*). The overall nucleotide sequence identity of 92% between SL-CoVs and SARS-CoVs is very similar to that observed between Nipah viruses isolated from Malaysia and Bangladesh in 1999 and 2004, respectively (*25*) (fig. S4). SL-CoVs present a new challenge to the diagnosis and treatment of future disease outbreaks. The current tests and therapeutic strategies may not work effectively against all viruses in this group, owing to their great genetic variability in the S1 domain region of the S gene.

The genus *Rhinolophus* contains 69 species and has a wide distribution from Australia to Europe (*27*). They roost primarily in caves and feed mainly on moths and beetles. However, notwithstanding the predominant *Rhinolophus* findings in this study, it is highly likely that there are more SARS-related coronaviruses to be discovered in bats. Indeed, our positive serological findings in the cave-dwelling fruit bat *Rousettus leschenaulti* indicate that infection by a related virus could occur in fruit bats as well, albeit at a much lower frequency. A plausible mechanism for emergence from a natural bat reservoir can be readily envisaged. Fruit bats including *R. leschenaulti*, and less frequently insectivorous bats, are found in markets in southern China. An infectious consignment of bats serendipitously juxtaposed with a susceptible amplifying species, such as *P. larvata*, at some point in the wildlife supply chain could result in spillover and establishment of a market cycle while susceptible animals are available to maintain infection. Further studies in field epidemiology, laboratory infection, and receptor distribution and usage are being conducted to assess potential roles played by different bat species in SARS emergence.

These findings on coronaviruses, together with data on henipaviruses (*23*–*25*, *28*), suggest that genetic diversity exists among zoonotic viruses in bats, increasing the possibility of variants crossing the species barrier and causing outbreaks of disease in human populations. It is therefore essential that we enhance our knowledge and understanding of reservoir host distribution, animal-animal and human-animal interaction (particularly within the wet-market system), and the genetic diversity of bat-borne viruses to prevent future outbreaks.

References and Notes

1. J. S. M. Peiris *et al.*, *Lancet* 361, 1319 (2003).
2. T. G. Ksiazek *et al.*, *N. Engl. J. Med.* 348, 1953 (2003).
3. P. A. Rota *et al.*, *Science* 300, 1394 (2003).
4. M. A. Marra *et al.*, *Science* 300, 1399 (2003).
5. Y. Guan *et al.*, *Science* 302, 276 (2003).
6. C. Tu *et al.*, *Emerg. Infect. Dis.* 10, 2244 (2004).
7. L. L. M. Poon *et al.*, *J. Virol.* 79, 2110 (2005).
8. D. Wu *et al.*, *J. Virol.* 79, 2620 (2005).
9. K. Murray *et al.*, *Science* 268, 94 (1995).
10. K. B. Chua *et al.*, *Science* 288, 1432 (2000).
11. L.-F. Wang, B. T. Eaton, *Infect. Dis. Rev.* 3, 52 (2001).
12. S. E. Sulkin, R. Allen, *Monograph Virol.* 8, 170 (1974).
13. S. P. Mickleburgh, A. M. Huston, P. A. Racey, *Oryx* 36, 18 (2002).
14. Materials and methods are available as supporting material on *Science* Online.
15. P. J. Hudson, A. Rizzoli, B. T. Grenfell, H. Heesterbeek, A. P. Dobson, Eds., *The Ecology of Wildlife Diseases* (Oxford Univ. Press, Oxford, 2002).
16. Chinese SARS Molecular Epidemiology Consortium, *Science* 303, 1666 (2004).
17. P. Liò, N. Goldman, *Trends Microbiol.* 12, 106 (2004).
18. H.-D. Song *et al.*, *Proc. Natl. Acad. Sci. U.S.A.* 102, 2430 (2005).
19. M. C. Lai, K. V. Holmes, in *Fields Virology*, D. M. Knipe *et al.*, Eds. (Lippincott, Williams & Wilkins, Philadelphia, 2001), vol. 2, chap. 35.
20. R. A. Tripp *et al.*, *J. Virol. Methods* 128, 21 (2005).
21. Y. He, H. Lu, P. Siddiqui, Y. Zhou, S. Jiang, *J. Immunol.* 174, 4908 (2005).
22. D. A. Brian, R. S. Baric, *Curr. Top. Microbiol. Immunol.* 287, 1 (2005).
23. S. AbuBakar *et al.*, *Emerg. Infect. Dis.* 10, 2228 (2004).
24. J.-M. Reynes *et al.*, *Emerg. Infect. Dis.* 11, 1042 (2005).
25. B. H. Harcourt *et al.*, *Emerg. Infect. Dis.* 11, 1594 (2005).
26. V. P. Hsu *et al.*, *Emerg. Infect. Dis.* 10, 2082 (2004).
27. T. H. Kunz, M. B. Fenton, Eds., *Bat Ecology* (Univ. of Chicago Press, Chicago, 2003).
28. L.-F. Wang, K. B. Chua, M. Yu, B. T. Eaton, *Curr. Genomics* 4, 263 (2003).
29. This work was jointly funded by a special grant for "Animal Reservoir of SARS-CoV," State Key Program for Basic Research Grant 2005CB523004, and State High Technology Development Program grant no.

2005AA219070 from the Ministry of Science and Technology, People's Republic of China; the Sixth Framework Program "EPISARS" from the European Commission (no. 51163); the Australian Biosecurity Cooperative Research Centre for Emerging Infectious Disease (Project 1.007R); and an NIH/NSF "Ecology of Infectious Diseases" award (no. R01-TW05869) from the John E. Fogarty International Center and the V. Kann Rasmussen Foundation. For the full-length genome sequence of SL-CoV Rp3, see GenBank accession no. DQ71615. Additional GenBank accession numbers are given in the supporting material.

Supporting Online Material
www.sciencemag.org/cgi/content/full/1118391/DC1
Materials and Methods
Figs. S1 to S4
Tables S1 to S3
References and Notes

4 August 2005; accepted 20 September 2005
Published online 29 September 2005;
10.1126/science.1118391
Include this information when citing this paper.

Neurogenesis in the Hypothalamus of Adult Mice: Potential Role in Energy Balance

Maia V. Kokoeva, Huali Yin, Jeffrey S. Flier*

Ciliary neurotrophic factor (CNTF) induces weight loss in obese rodents and humans, and for reasons that are not understood, its effects persist after the cessation of treatment. Here we demonstrate that centrally administered CNTF induces cell proliferation in feeding centers of the murine hypothalamus. Many of the newborn cells express neuronal markers and show functional phenotypes relevant for energy-balance control, including a capacity for leptin-induced phosphorylation of signal transducer and activator of transcription 3 (STAT3). Co-administration of the mitotic blocker cytosine-β-D-arabinofuranoside (Ara-C) eliminates the proliferation of neural cells and abrogates the long-term, but not the short-term, effect of CNTF on body weight. These findings link the sustained effect of CNTF on energy balance to hypothalamic neurogenesis and suggest that regulated hypothalamic neurogenesis in adult mice may play a previously unappreciated role in physiology and disease.

The obesity epidemic has prompted major efforts to develop safe and effective therapies (*1*, *2*). However, approved drugs for obesity have limited efficacy and act only acutely, with patients rapidly regaining weight after terminating treatment (*3*). Only the neurocytokine ciliary neurotrophic factor (CNTF) and Axokine, an analog of CNTF developed as a drug candidate for the treatment of obesity, appear to deviate from this paradigm. Rodents and patients treated with Axokine were reported to maintain lowered body weights weeks to months after the cessation of treatment (*4*, *5*). This feature of Axokine/CNTF action is unexplained and suggests that CNTF induces long-lasting changes in one or more elements of the energy-balance circuitry.

In rodents, CNTF is most potent when administered directly into the cerebrospinal fluid (*6*) and activates signaling cascades in hypothalamic nuclei involved in feeding control (*5*, *7*, *8*). For instance, CNTF activates phosphorylation of signal transducer and activator of transcription 3 (STAT3) in a population of hypothalamic neurons that substantially overlaps with those activated by leptin (*5*). However, in contrast to CNTF, leptin-treated animals do not maintain their lowered body weight after the cessation of treatment. We thus sought a CNTF-specific mechanism to explain this long-term effect.

CNTF supports the survival of neurons in vitro and in vivo (*9*) and has also been implicated in the maintenance of adult neural stem cells (*10*). Furthermore, other trophic factors, such as epidermal growth factor and fibroblast growth factor 2, are known to act as mitogens on adult neuronal progenitors (*11*, *12*), and they promote the functional regeneration of hippocampal pyramidal neurons (*13*). Neurogenesis in the adult brain is most clearly defined in the subventricular zone (SVZ) of the lateral ventricles and the subgranular zone (SGZ) of the hippocampal formation (*14*). However, recent reports indicate that the neuroproliferative potency in the adult extends to other brain structures, including the hypothalamus (*15*–*17*). On the basis of these findings, we hypothesized that the long-term effect of CNTF on body-weight regulation might involve neurogenesis in the hypothalamus, which is the brain region most relevant for energy-balance regulation.

To assess the mitogenic potency of CNTF in the adult nervous system in vivo, we delivered the cell-proliferation marker bromodeoxyuridine (BrdU) alone (vehicle treatment) or together with CNTF directly into the cerebrospinal fluid of mouse brains (*18*). CNTF and BrdU were continuously infused for 7 days into the right lateral ventricle using osmotic minipumps. Mice were switched to a high-fat diet two months before surgery and were kept on this diet throughout the experiments. In accordance with previous results (*5*), CNTF-treated mice showed a marked reduction in body weights (Fig. 1A), which persisted after termination of CNTF delivery. Mice were killed 22 days after surgery, and brain sections were immunostained with an antibody against BrdU. Because BrdU incorporates into DNA of dividing cells, BrdU-positive (BrdU$^+$) cells are thought to represent newborn cells. Figure 1B shows coronal sections of vehicle- and CNTF-infused animals at the level of the arcuate, ventromedial, and dorsomedial nuclei, well-known hypothalamic centers for energy-balance regulation (*19*). In vehicle-infused animals, few BrdU$^+$ cells were detected in the parenchyma surrounding the third ventricle (Fig. 1B, left). Administration with CNTF led to a dramatic increase of BrdU+ cells (Fig. 1B, right). Note the higher density of BrdU$^+$ cells at the base of the third ventricle, which is part of the arcuate nucleus/median eminence.

The pattern of CNTF receptor (CNTFR) mRNA expression is consistent with this observation. In situ hybridization using a riboprobe against CNTFR mRNA revealed strong staining in the walls of the basal third ventricle and surrounding arcuate nucleus parenchyma (Fig. 1C). Because this section originated from an animal treated with both CNTF and BrdU, we colabeled with antibodies to BrdU. Many BrdU$^+$ cells were positive for CNTFR expression, indicating that CNTF, at least in part, directly promotes cell division by binding to CNTFR on putative neural progenitor cells (Fig. 1D, inset). By counting all newly generated cells in the caudal hypothalamus, CNTF treatment led to a marked increase of BrdU$^+$ cells over vehicle-infused animals (Fig. 1E). The total number of BrdU$^+$ cells in CNTF-treated animals remained constant for at least 2 weeks after the infusion period. Subsequently, the numbers decreased but plateaued at a high level. Vehicle-infused animals showed a similar fractional decrease over time. Thus it appears that the majority of hypothalamic BrdU$^+$ cells do not die or migrate to distant areas as reported for newborn neurons of the SVZ, which follow the rostral migratory stream toward the olfactory bulb (*20*).

To investigate the origin of adult-born cells in the hypothalamus, we examined CNTF and vehicle-infused brains every 12 hours starting 48 hours after surgery, a time when the infused CNTF/BrdU should just reach the ventricular system (*18*). Hypothalamic BrdU incorporation was first detected 60 to 72 hours

Division of Endocrinology, Department of Medicine, Beth Israel Deaconess Medical Center and Harvard Medical School, 99 Brookline Avenue, Boston, MA 02215, USA.

*To whom correspondence should be addressed. E-mail: jflier@bidmc.harvard.edu